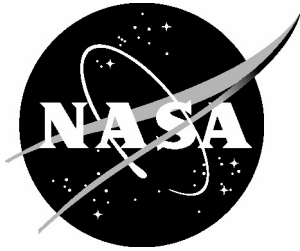


NASA/TM-2004-213262
ARL-TR-3233



Experimental Results From Stitched Composite Multi-Bay Fuselage Panels Tested Under Uni-Axial Compression

Donald J. Baker
U.S. Army Research Laboratory
Vehicle Technology Directorate
Langley Research Center, Hampton, Virginia

The NASA STI Program Office . . . in Profile

Since its founding, NASA has been dedicated to the advancement of aeronautics and space science. The NASA Scientific and Technical Information (STI) Program Office plays a key part in helping NASA maintain this important role.

The NASA STI Program Office is operated by Langley Research Center, the lead center for NASA's scientific and technical information. The NASA STI Program Office provides access to the NASA STI Database, the largest collection of aeronautical and space science STI in the world. The Program Office is also NASA's institutional mechanism for disseminating the results of its research and development activities. These results are published by NASA in the NASA STI Report Series, which includes the following report types:

- **TECHNICAL PUBLICATION.** Reports of completed research or a major significant phase of research that present the results of NASA programs and include extensive data or theoretical analysis. Includes compilations of significant scientific and technical data and information deemed to be of continuing reference value. NASA counterpart of peer-reviewed formal professional papers, but having less stringent limitations on manuscript length and extent of graphic presentations.
- **TECHNICAL MEMORANDUM.** Scientific and technical findings that are preliminary or of specialized interest, e.g., quick release reports, working papers, and bibliographies that contain minimal annotation. Does not contain extensive analysis.
- **CONTRACTOR REPORT.** Scientific and technical findings by NASA-sponsored contractors and grantees.

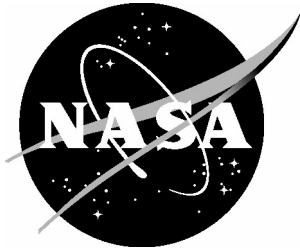
- **CONFERENCE PUBLICATION.** Collected papers from scientific and technical conferences, symposia, seminars, or other meetings sponsored or co-sponsored by NASA.
- **SPECIAL PUBLICATION.** Scientific, technical, or historical information from NASA programs, projects, and missions, often concerned with subjects having substantial public interest.
- **TECHNICAL TRANSLATION.** English-language translations of foreign scientific and technical material pertinent to NASA's mission.

Specialized services that complement the STI Program Office's diverse offerings include creating custom thesauri, building customized databases, organizing and publishing research results ... even providing videos.

For more information about the NASA STI Program Office, see the following:

- Access the NASA STI Program Home Page at <http://www.sti.nasa.gov>
- E-mail your question via the Internet to help@sti.nasa.gov
- Fax your question to the NASA STI Help Desk at (301) 621-0134
- Phone the NASA STI Help Desk at (301) 621-0390
- Write to:
NASA STI Help Desk
NASA Center for AeroSpace Information
7121 Standard Drive
Hanover, MD 21076-1320

NASA/TM-2004-213262
ARL-TR-3233



Experimental Results From Stitched Composite Multi-Bay Fuselage Panels Tested Under Uni-Axial Compression

Donald J. Baker
U.S. Army Research Laboratory
Vehicle Technology Directorate
Langley Research Center, Hampton, Virginia

National Aeronautics and
Space Administration

Langley Research Center
Hampton, Virginia 23681-2199

September 2004

The use of trademarks or names of manufacturers in the report is for accurate reporting and does not constitute an official endorsement, either expressed or implied, of such products or manufacturers by the National Aeronautics and Space Administration or the U.S. Army.

Available from:

NASA Center for AeroSpace Information (CASI)
7121 Standard Drive
Hanover, MD 21076-1320
(301) 621-0390

National Technical Information Service (NTIS)
5285 Port Royal Road
Springfield, VA 22161-2171
(703) 605-6000

Abstract

The experimental results from two stitched VARTM carbon-epoxy composite panels tested under uni-axial compression loading are presented. The curved panels are divided by frames and stringers into five or six bays with a column of three bays along the compressive loading direction. The frames are supported at the frame ends to resist out-of-plane translation. Back-to-back strain gages are used to record the strain and displacement transducers were used to record the out-of-plane displacements. In addition a full-field-displacement measurement technique that utilizes a camera-based-stereo-vision system was used to record the displacements. The panels were loaded in increments to determine the first bay to buckle. Loading was discontinued at limit load and the panels were removed from the test machine for impact testing. After impacting at 20 ft-lbs to 25 ft-lbs of energy with a spherical indenter, the panels were loaded in compression until failure. Impact testing reduced the axial stiffness by 4 percent and less than 1 percent. Post-buckled axial panel stiffness was 52 percent and 70 percent of the pre-buckled stiffness.

Introduction

To improve the cost and weight savings of composite helicopter structures it will be necessary to reduce the conservatism that is used now in the design and analysis process. As part of SARAP (Survivable, Affordable, Repairable Airframe Program), Boeing – Helicopters is developing a high fidelity failure analysis methodology to analyze unitized composite structures. This high fidelity failure analysis methodology address the limitations of current strength analysis used in the design process. Potential failure modes missed by the present strength analysis can be identified with the high fidelity analysis before full-scale tests are conducted. To assist in the validation, Boeing supplied two panels that were cut from a RWSTD (Rotary Wing Structures Technology Demonstrator) composite tool proof article for testing by Vehicle Technology Directorate (VTD). This testing supports SARAP Task 1.2.4 “Structural Technology” by validating the high fidelity failure analysis and Task 1.2.5 “Durability and Damage Tolerance” effect of barely visible damage on compression failure.

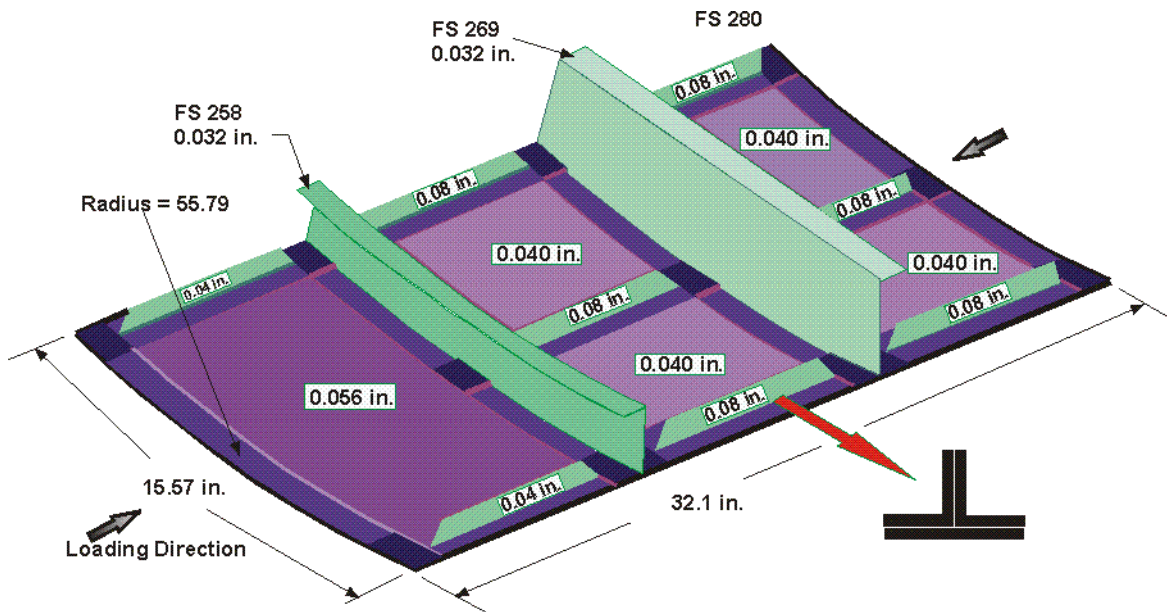
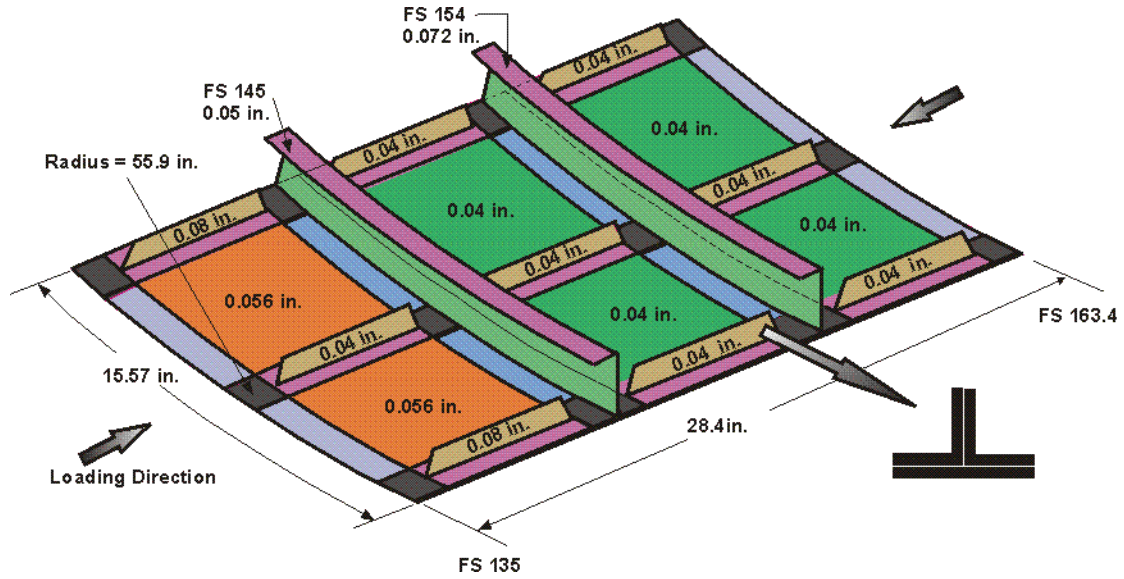
Two panels were cut from a stitched VARTM carbon-epoxy composite fuselage section that was used to verify a manufacturing tool. Each panel contains two frames and three stringers. The frames and stringers divide one panel into six bays which will be identified as *Panel C-1* in the remainder of the paper. There are two columns of three bays each in the compressive loading direction. The other panel to be identified as *Panel C-2* has a stringer on the centerline of the panel omitted between a frame and the end of the panel thus producing a panel with 5 bays.

The objective of this report is to present the experimental data from the composite panels tested by VTD.

Test panels

Details of the stitched VARTM composite *Panel C-1* supplied by Boeing are shown in Figure 1. The skin is stitched together and the frame and stringer flanges are stitched to the skin. The panel is 15.57-inches wide with a 55.9-inch radius in the width direction. The stringer leg terminates before the frame flange of each frame while the flanges from the stringer continues under the frame flange. The panel ends were potted with 1-inch thick filled epoxy and were machined flat and parallel to the 28.4-inch dimension shown in Figure 1. A 1-inch long section of the frame flange located at FS 145 and 154 was removed from each end. A 1-inch square, 0.062-inch thick, aluminum plate was bonded to each side of the web for reinforcement for frame to resist the out-of-plane displacement at the frame ends.

Test *Panel C-2* is very similar to *Panel C-1* with an overall length of 32.1-inches between the potted ends as shown in Figure 2. The middle stringer does not extend between FS 247.7 and FS 258 thus producing a panel with five bays. Also note that Frame 269 is much deeper than frame FS 258. The specimen was prepared for test the same as for Panel C-1.



Test Plan

The test plan for each panel is as follows:

Panel C-1

- Load to 1,000 lbs for instrumentation checkout.
- Load to 3,950 lbs with free edges to determine initial buckling.
- Load to 5,515 lbs with knife edges on free edges between frames to determine the initial buckling load
- Remove *Panel C-1* from test setup and impact with dropped weight impactor at 20 ft-lbs energy.
- Reinstall panel in test setup and load until failure.

Panel C-2

- Load to 4,000 lbs with knife edges on the free edges to determine initial buckling.
- Load to 4,500 lbs with knife edges on the free edges to determine initial buckling.
- Remove *Panel C-2* from test setup and impact with a dropped weight impactor at 20 ft-lbs of energy.
- Reinstall panel in test setup and load until failure.

Instrumentation

Three measurement techniques were utilized to determine the response of these panels.

Strain gages – Common off the shelf axial and rosette strain gages were used on the panels. *Panel C-1* contained 42 strain gages – back-to-back rosettes in the center of each bay and back-to-back axial gages across the center of the specimen as shown in Figure 3. *Panel C-2* contained 36 strain gages – back-to-back rosettes in the center of each bay and back-to-back axial gages across the center of the specimen as shown in Figure 3.

Displacement transducers – Linear variable displacement transducers (LVDT) were utilized to measure the displacements at selected locations shown in Figure 3. In addition to the LVDT shown in Figure 3 two LVDT's were used to measure the panel end shortening.

3-D Vision Correlation System (VIC-3D) - This system is a full-field-displacement measurement technique [1] that utilizes a camera-based stereo-vision system. VIC-3D¹ is a non-intrusive system that uses a black spackle pattern on a white background applied to the specimen to establish the specimen displacement tracking points. Images of the changing pattern on the test specimen surface are recorded on a computer with the stereo-vision system at user specified time intervals. It is also possible take data

¹VIC-3D system supplied by Correlated Solutions, Inc., W. Columbia, SC

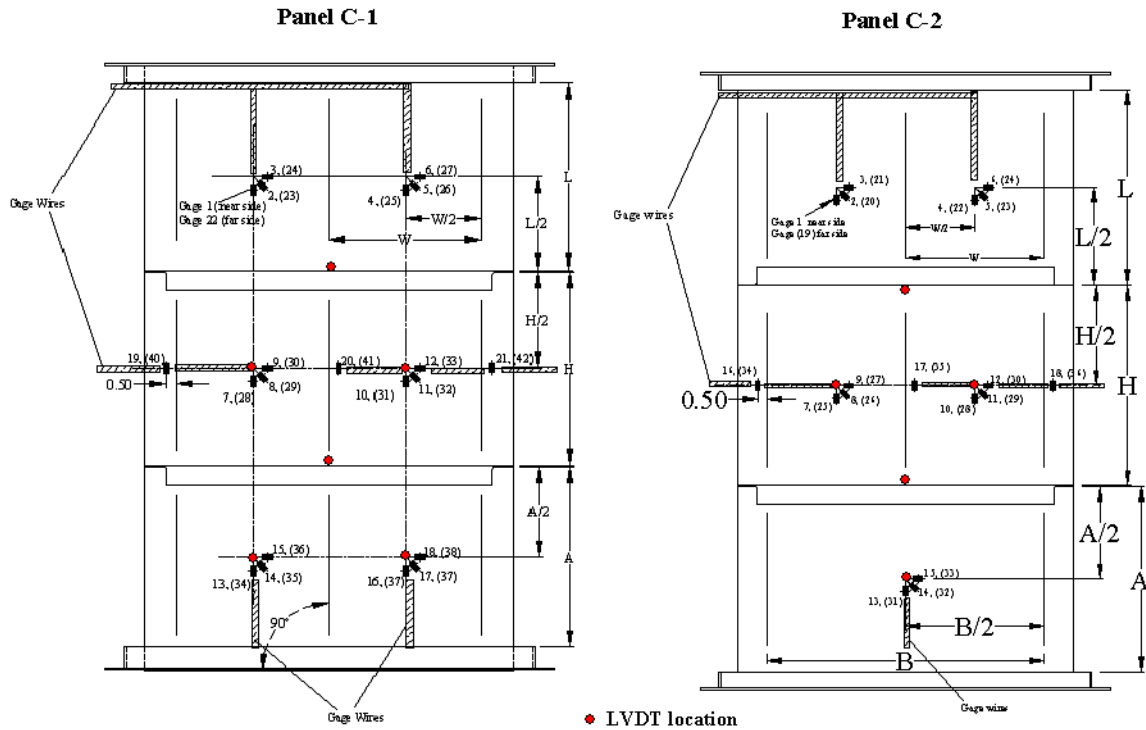


Figure 3. Strain gage and DCDT locations.

in a local area with a second camera based system while taking data on a global area. This will give higher resolution to an area of interest.

Results and Discussion

Panel C-1

An analysis and comparison to transducer results for *Panel C-1* is presented in Reference [2].

The left hand side of Figure 4 shows *Panel C-1* installed in the test machine. The frame to react the out-of-plane panel frame loads is shown. This frame is attached to the test machine lower platen and reacts the panel frame out-of-plane loads but not frame rotations. The linkage from the panel allows the test specimen frames to rotate but not translate.

The speckle pattern used for the VIC 3-D system can be seen in the L/H side of Figure 4. The skin surface of the test specimen was painted white then the black speckle pattern was applied. Note the different speckle densities can be seen between the local and global area, where the local has smaller speckles and a higher density. The local area location was selected to encompass the future impact site.

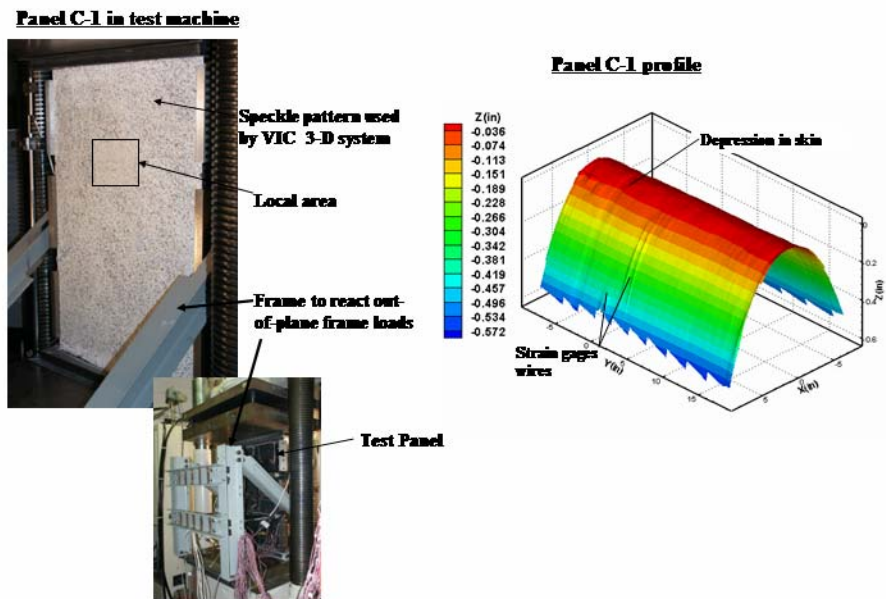


Figure 4. - *Panel C-1* in test machine and profile view of panel.

The right hand side of Figure 4 shows the profile of *Panel C-1*. The specimen profile is determined from the first image taken by the VIC-3D system before any load application. A best fit flat plane is fit to the data points in the first image. There are usually 8,000 to 10,000 data points used to determine the best fit plane. Then the distance from the best fit plane to the panel surface is determined and a new surface is plotted that reflects any defects. The profile of *Panel C-1* does not indicate any significant defects. A small depression in the skin is indicated. These defects produce very small ripples in lines of constant distance when plotting the contours from the best fit plane. A strain gages and associated wiring can also be seen in the picture.

Figure 5 summarizes some of the data from the first test on *Panel C-1* where the load was taken to $N_y = 3,950$ lbs, a point just past the predicted first buckle for a specimen with free edges. The perspective view in the upper L/H corner of Figure 5 is the out-of-plane displacements at a load of $N_y = 3,899$ lbs. indicating a buckle in the upper R/H bay and the other bays bulging out-of-plane. For the remainder of this report the bay identifications are located relative to looking at the skin side of the panel and a positive displacement is defined as displacement toward the viewer. The pictures of the w displacement (upper R/H in the figure) have been cropped to show only the upper R/H skin bay. The out-of-plane displacements shown for $N_y = 3,340$ lbs indicates the skin panel is starting to bulge out-of-plane (positive direction) as two bulges prior to going to a single half-wave in the negative direction as shown in the figure for a load of $N_y = 3,575$ lbs.

The results from axial back-to-back strain gages in the center of the upper R/H skin bay are shown in lower L/H corner of the Figure. The strain results indicate skin bending started at approximately $N_y = 2,000$ lbs. and continued until buckling occurred at approximately $N_y = 3,500$ lb.

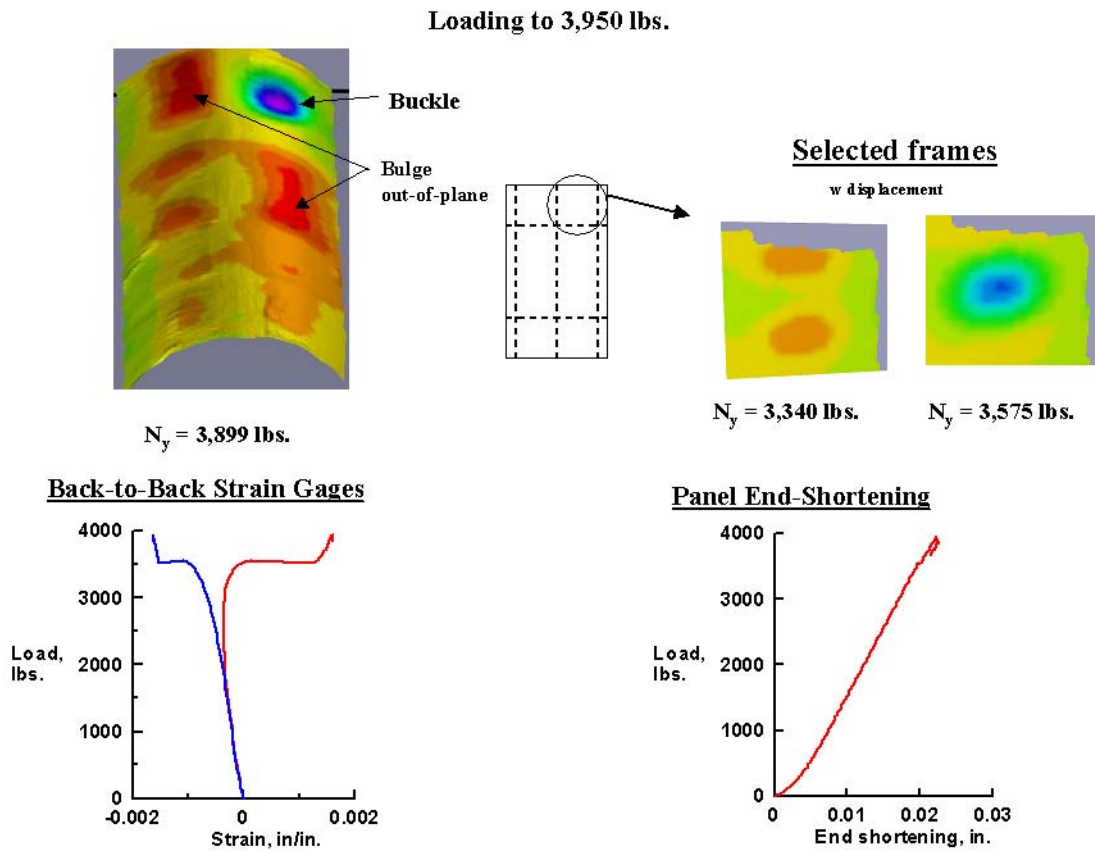


Figure 5. - Results from load Panel C-1 to 3,950 lbs.

The panel end shortening as a function of the applied load is shown in the lower R/H corner of Figure 5. The response appears to be linear after initial loading until the skin buckles. After buckling the response appears to be linear but at a lower slope than the initial response.

Knife edges were attached to the free skin edges for the second test on *Panel C-1* and the maximum load was increased to $N_y = 5,515$ lbs, which is more than the predicted buckling load. A buckle develops in the upper R/H corner of the specimen as shown in the upper R/H side of Figure 6. As the load was increased a buckle developed in center bay, L/H side, as shown in the upper L/H side of Figure 6. The first buckle occurred at a load a few pounds higher than in the first test as can be seen when comparing this result with the result on the previous figure. The second buckle occurred at approximately a 200 lbs. higher load than the first buckle.

The load as a function of the end-shortening is shown in the center of Figure 6 and is the same as the curve for the first test with different slopes before and after the skin buckling. The response appears to be linear after initial loading until the skin buckles. After buckling the response appears to be linear but at a lower slope than the initial response. The initial (before first buckle) slope of this curve is approximately 2 percent higher than the slope of the end shortening curve for a panel without knife edges.

The addition of knife edges to the skin free edges did not have a significant effect on the buckling loads. The specimen was removed from the test machine for impacting.

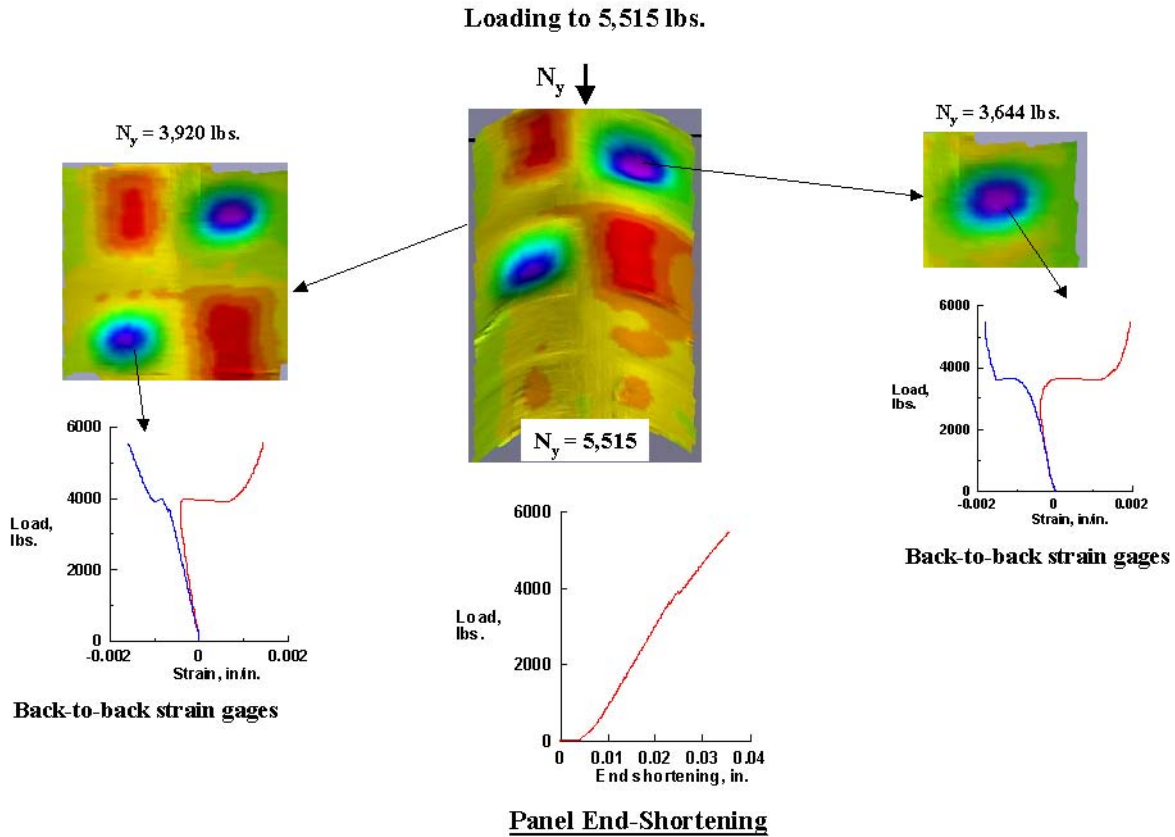


Figure 6. - Results of loading *Panel C-1* to $N_y = 5,515$ lbs.

Panel C-1 was placed under the impact tower shown in Figure 7 and a 5-lb weight with a 0.5-inch spherical radius indenter was dropped on the specimen. One-hundred pounds of lead shot was placed on and around the specimen to damp the vibrations.

Impact location was to be on panel centerline at the end of stringer 9, in the skin and stringer flange thickness adjacent to FS 154 frame flange. The impactor was dropped 4-ft to give an impact energy of 20 ft-lbs. Barely visible impact damage occurred on the specimen with the 20 ft-lbs of impact energy. A photograph of the impact site with the actual impact location is shown in Figure 7. The contact force profile shown in Figure 7 indicated a loss of stiffness as given by the contact force drop of approximately 150 lbs. after reaching the peak force of 908 lbs. The contact force recovered some but never greater than the peak value of 908 lbs.

Panel C-1 was returned to the test machine for testing to failure. The profile of a 4.0-inch by 4.0-inch area around the impact site, taken using VIC-3D local cameras, indicated the impact dent depth to be 0.008 to 0.010-inches deep from the surrounding surface. The surface depression in the skin, noted on Figure 4, is also evident in the profile shown in Figure 7.

For this test *Panel C-1* was loaded to failure. A view of the out-of-plane displacement (top – center of Figure 8) is shown for $N_y = 5,633$ lbs, near the failure load of $N_y = 5,678$ lbs. Strain gage results for the three panels that buckled during test are shown in Figure 8. The bay on the upper L/H bulged as the

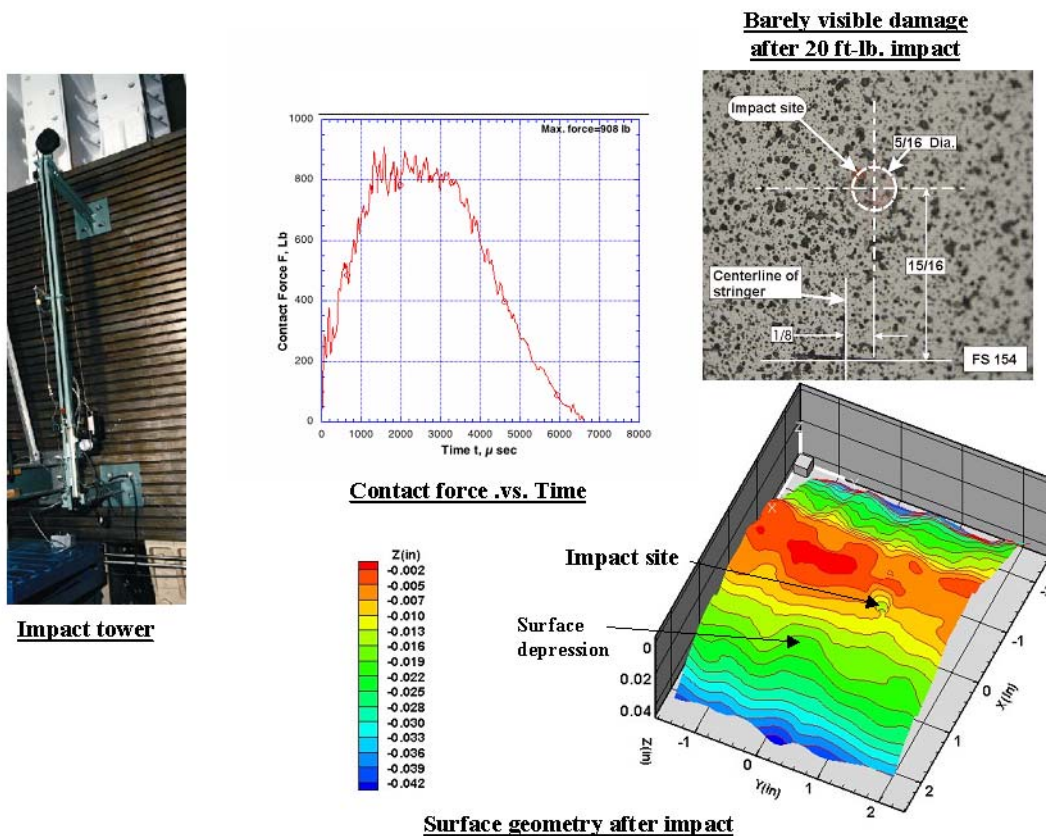


Figure 7. - Impact test results on *Panel C-1*.

load increased until approximately $N_y = 5,000$ lb. at which time the skin started to bend. The first indication of buckling was in the upper R/H bay with the buckle starting at $N_y = 3,452$ lb. The load dropped to $N_y = 3,421$ lbs before increasing. The second buckle appeared in the middle L/H bay at $N_y = 3,763$ lbs. The load dropped to $N_y = 3,709$ lbs before starting to increase. As the load increased to approximately 5,500 lbs. the buckles get deeper. Selected events from $N_y = 2,000$ lbs. to failure are shown in the next figure.

The load shortening curve indicates a linear response until initial panel buckling and then linear response after the second panel buckled until near failure. The slope of the curve (from 1,500 lbs to 3,500 lbs) is 4 percent less than the curve shown in Figure 6, indicating that the impact damage has a small effect on the panel axial stiffness. The slope of the curve after the buckling (post buckling stiffness) is 70 percent of the initial slope.

Figure 9 presents a series of out-of-plane (w) displacement contour plots as the load is increased. The top L/H picture for $N_y = 2,031$ lbs indicates 5 of the 6 bays with similar w displacements of up to 0.009 inches. The upper R/H bay indicated w displacements of up to 0.004 inches. All bays appears to have 2 bulges. The dashed lines on the pictures are the approximate locations of the frames and stringers. Increasing the load to $N_y = 3,214$ lbs. increases the maximum w displacements to 0.017 inches on 3 of the panels while the other 3 panels increase to 0.010 to 0.013 inches. In addition a negative displace-

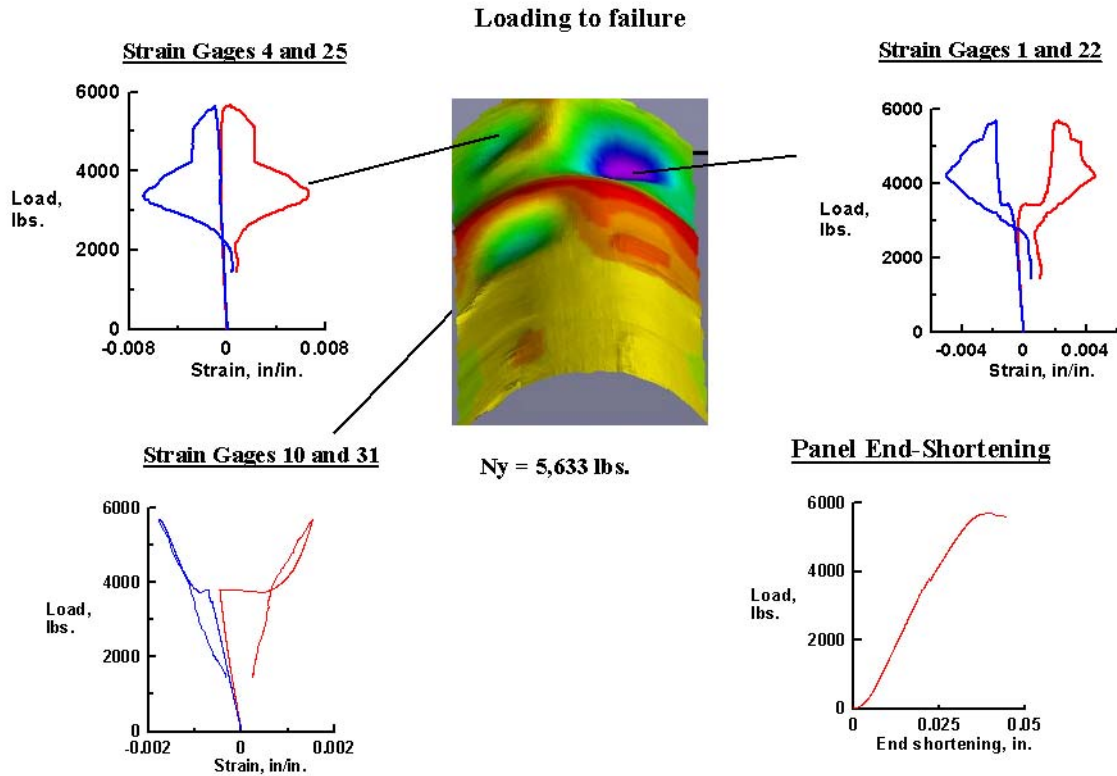


Figure 8. - Test result summary for selected strain gages on *Panel C-1*.

ment (-0.002 inch) appears in the upper R/H panel and is shown as Point “A” in the detail in the center of the top row.

Increasing the load to $N_y = 3,320$ lbs. increases the magnitudes of the displacement by 0.001 inch. Increasing the load to $N_y = 3,472$ lbs. increases the w displacements to +0.018 to -0.008-inches. The next picture (first on the bottom row) is the next frame of data taken (approximately 10 second interval). The upper R/H bay has buckled in a half wave that has a -0.062-inch of displacement. The maximum displacement in the red shaded area is +0.025-inches. A half-wave buckle develops in the middle L/H side bay near $N_y = 3,712$ lbs. Increasing the load increases the out-of-plane deformation as shown by the figure for a load of $N_y = 5,345$ lbs. The deformation range is now +0.047-inches to -0.190-inches. The image at $N_y = 5,655$ lbs. indicates a mode shape change occurring in the upper L/H bay. The upper L/H panel changes into a half wave as shown in the next picture. When this happens the skin loses its load carrying capability and the specimen folds across at the frame. The last picture indicates the specimen has lost approximately 600 lbs in load carrying capability.

VIC-3D analysis software also has the capability to extract local data from the recorded images. Options exist that allow extraction of displacement and/or strain results at a point in the image or along a line on the image. The origin of the coordinate system has been selected as the intersection of the center stiffener and FS 145 as shown in Figure 10 on the out-of-plane displacement contour plot of *Panel C-1* for a load of $N_y = 5,345$ lbs. Selecting Line A through the impact site as shown in the Fig. 10 will

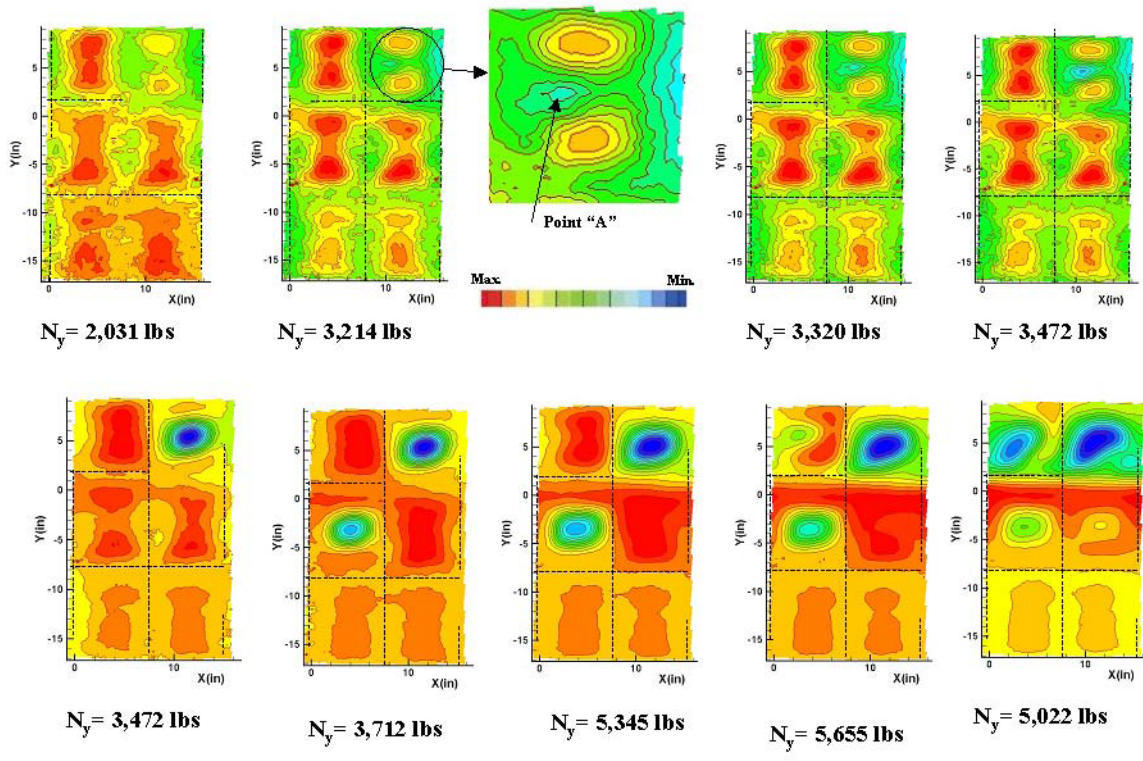


Figure 9. - Out-of-plane displacement history for *Panel C-1*.

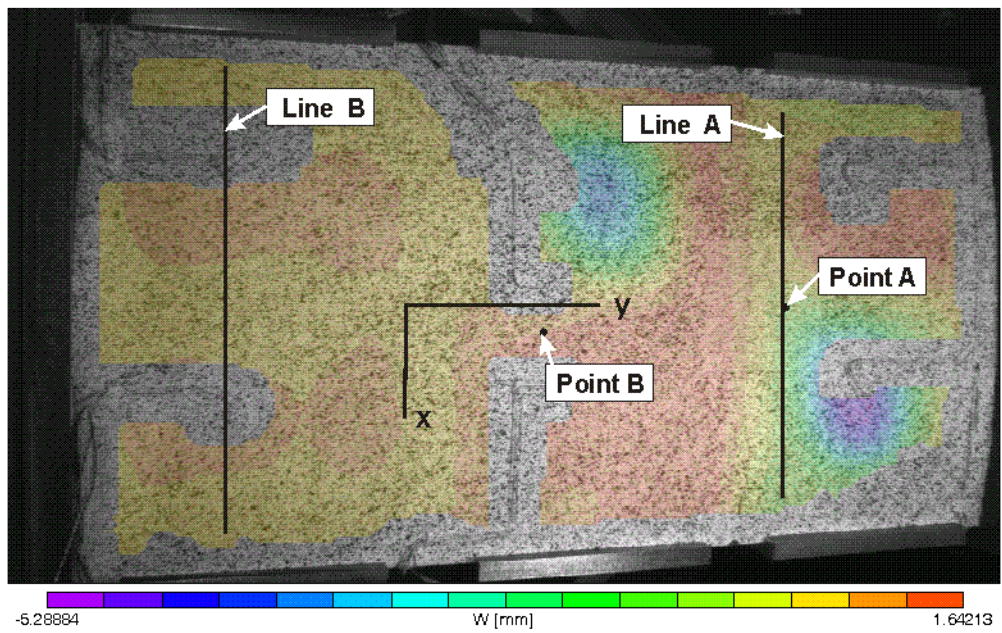


Figure 10. Out-of-plane contour plot and location of selected strain and displacement results for *Panel C-1*.

give the profile of the panel cross-section and the out-of-plane, w , displacements at 100 points (number of points selected by user) across the panel. The location of this line is approximated by selecting two points on the screen. At the present it is not possible to select this line or any point in direct relation to the specimen reference frame. Selecting the points on the screen is the only method. The profile of the panel, at Line A, after impact damage is shown in Figure 11. The distances shown in the Figure are the distance from a theoretical flat plane to the surface of the specimen. The dent from the impact is not obvious in Figure 11. A small variation in the curve near the top is probably the effect from the dent. A dent of 0.008-inch to 0.010-inch deep would not show up as a significant deviation in the curve considering the scale of the y-axis. The out-of-plane displacement results at the location of Line A shown in Fig. 10 are shown in Fig 12 for selected loads that vary from $N_y = 3,009$ lbs. to $N_y = 5,655$ lbs, which is the image near the maximum load. The panel appears to rotate about the side $x = -8.0$ -in. where the out-

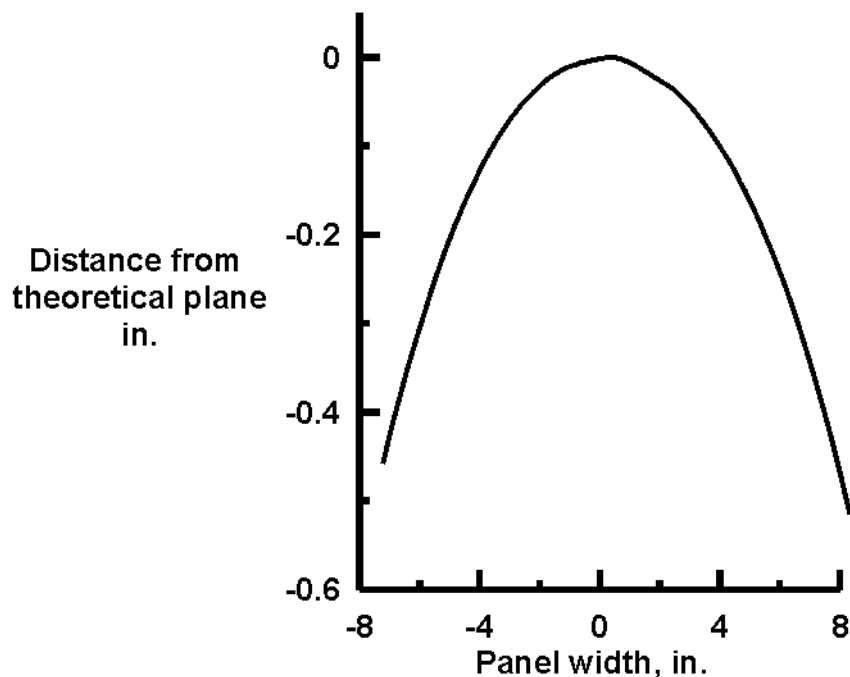


Figure 11. Profile of *Panel C-1* across the panel at Line A.

of-plane displacement varies less than 0.01-in. for the load less than $N_y = 5,345$ lbs. while the side at $x = 8.0$ -in. moves approximately 0.03-in. These curves also indicate how the bays deflect with load. The upper L/H bay deflects in the positive direction while the upper R/H bay deflects in the negative direction. Point A (Figure 10) was selected at the impact site. Again this point has been selected from picking a point on the screen which can lead to some error in the location. The load-out-of-plane displacement history is shown in Figure 13 for loading before and after impacting the panel. Also included in Figure 13 are the results from the test to failure for LVDT 16 which is located below the impact site and on the flange of the frame. The slope of the load-displacement curves before and after impacting are very similar up to 3,000 lbs. From 3,000 lbs to 3,500 lbs the after impact curve has larger displacement than the before impact curve. The displacement at LVDT 16 follows the same trend as the displacement curves for the impact site.

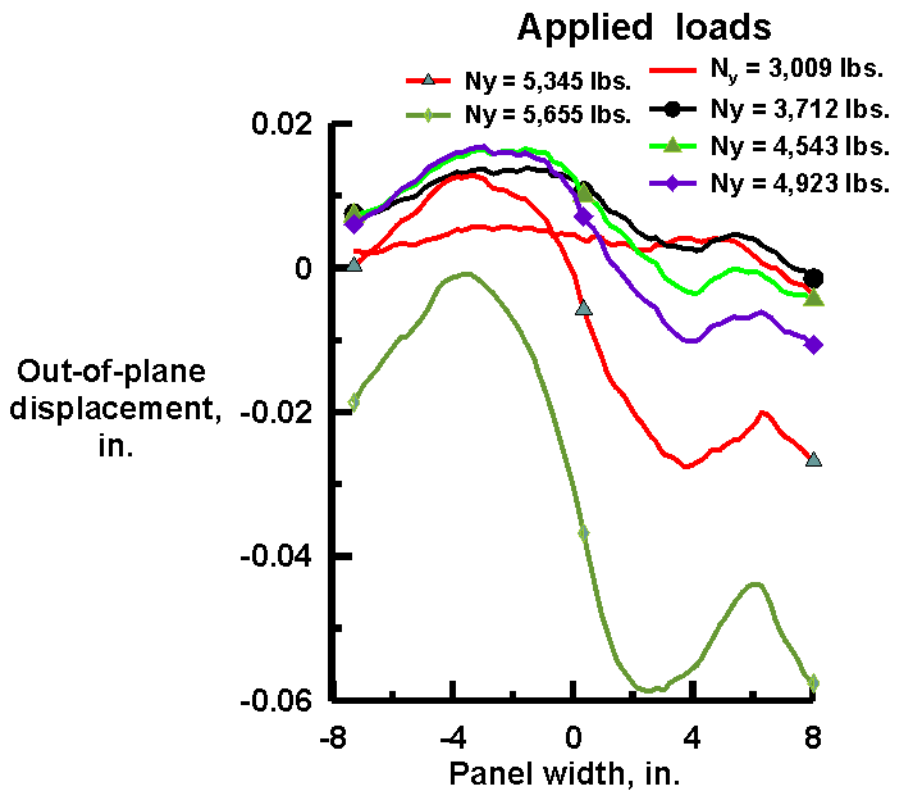


Figure 12 History of out-of-plane displacements for Panel C-1 as a function of applied load.

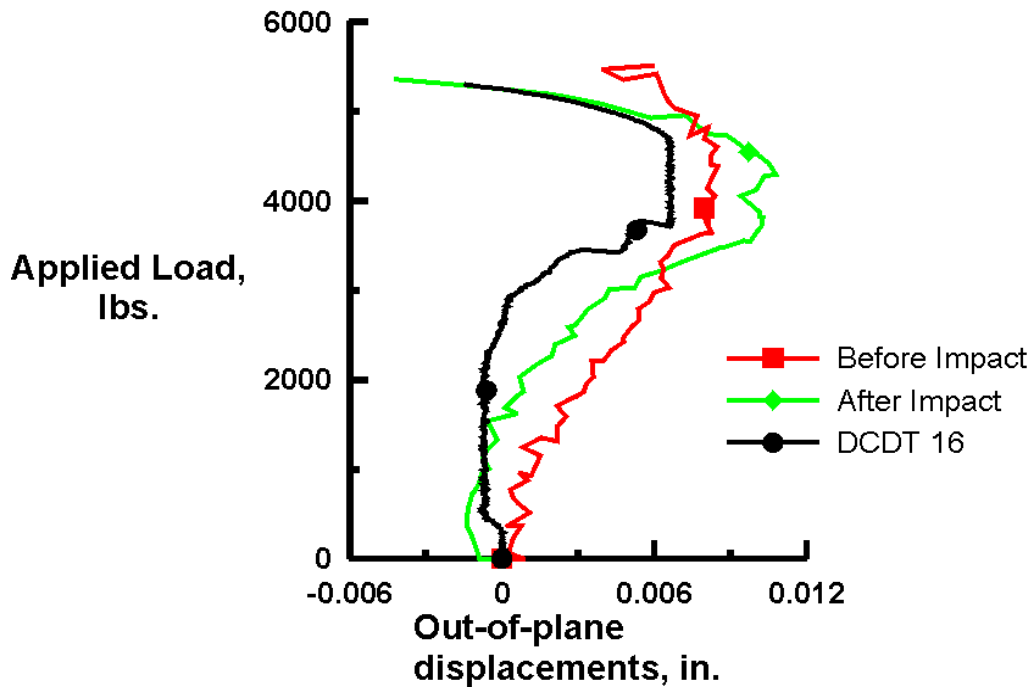


Figure 13. Out-of-plane displacements before and after impacting of Panel C-1.

VIC-3D software also has the capability of extracting strain from the images at a point or along a line. The first strain to be extracted from the images will be along Line B shown Figure 10. This line crosses at the centers of two bays (lower L/H and lower R/H) at the location of the strain rosettes. The strain results for $N_y = 5,345$ lbs are shown in Figure 14 as a line of blue circles. The missing sections of

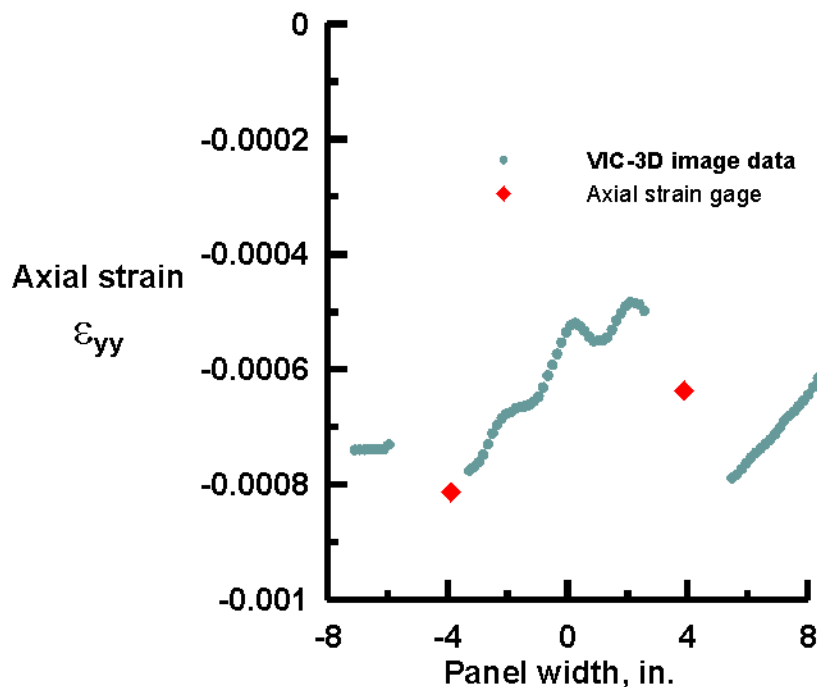


Figure 14. - Strain at Line B in the skin for $N_y = 5,345$ lbs.

the curve shown in Figure 14 are the locations of the rosettes. It is necessary to remove areas in the images where the rosettes are located due to the surface being non-flat from the gages and associated circuitry. The red diamonds shown in Figure 14 are the strain values recorded by the axial gages of the rosettes in the center of each bay. A good comparison exists for the two methods of measuring strain. This analysis software also has the capability of determining the strain at a point as a function of image number or load. Strain in skin at Point B (Figure 10) is shown in Figure 15 as small filled circles. The strain result at gage 20 (Figure 3), which is adjacent to Point B, is also shown in Figure 15. Good comparisons exist between the two strain measuring methods for a loads less than 1,800 lbs and greater than 4,200 lbs.

A photograph of the failed specimen in the test machine is shown on the L/H side of Figure 16 and is still under some load. It can be seen where the panel folded in the skin adjacent to the flange of the frame at FS 154. The edge view detail shows the out-of-plane displacement. The impact site is in the failure line. Close up photographs of the area at the impact site indicate cracks/crazing radiating from the impact site.

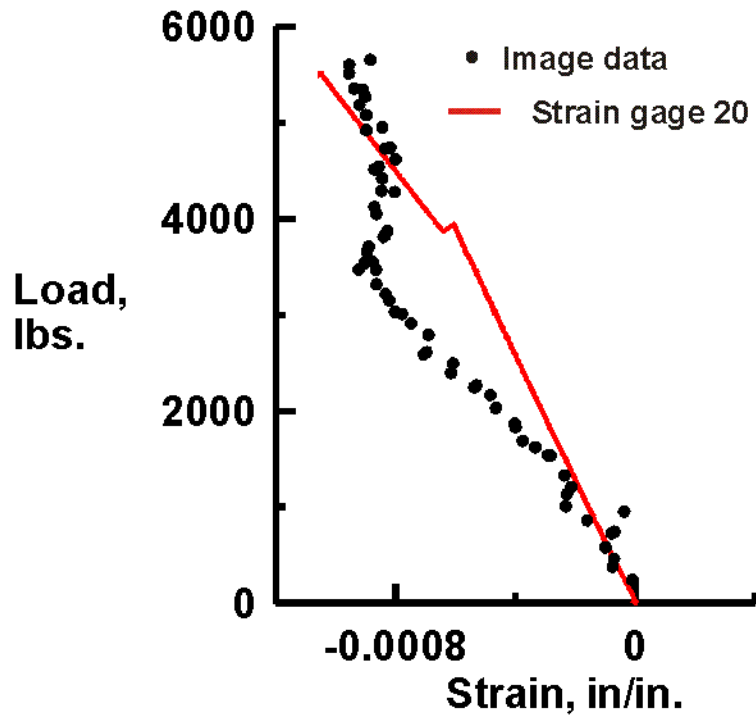


Figure 15. - Strain at Point B in the skin for $N_y = 5,345$ lbs.

Max load = 5,678 lbs.

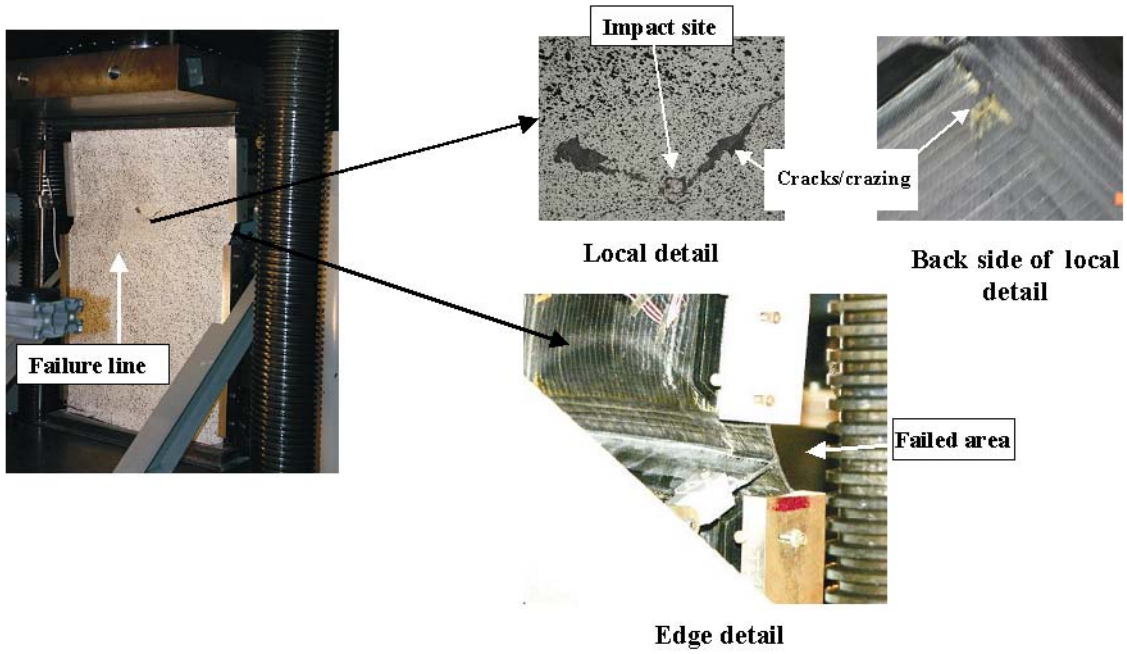


Figure 16. - Failed *Panel C-1*

Panel C-2

The first image taken by the VIC-3D system is used to determine the specimen profile. The perspective view of *Panel C-2* shown on the left side of Figure 17 is the profile of the panel before any load is applied. The contours shown are the distances from a theoretical flat plane. The only imperfection that is indicated in the panel is a depression in the skin near FS 269 frame. The imperfection is also extends to the side of the panel not shown in the view. A better local view shown later indicates the imperfection is approximately 0.02-inches below the surrounding surface. A set of strain gage leads also appears in the panel profile.

On the right side of Figure 17 is the out-of-plane displacements on the first loading of *Panel C-2* to determine a buckling load. The image shown was taken at a load of $N_y = 3,992$ lbs. No buckling was observed in the loading to 4,000 lbs. The bottom bay of the specimen bulges as shown by the red area. The image indicates two peaks, 0.030-in. to 0.033-in. high in the bulge. The strain gage results also indicate the lower bay loaded in compression with a small bending, but no buckling.

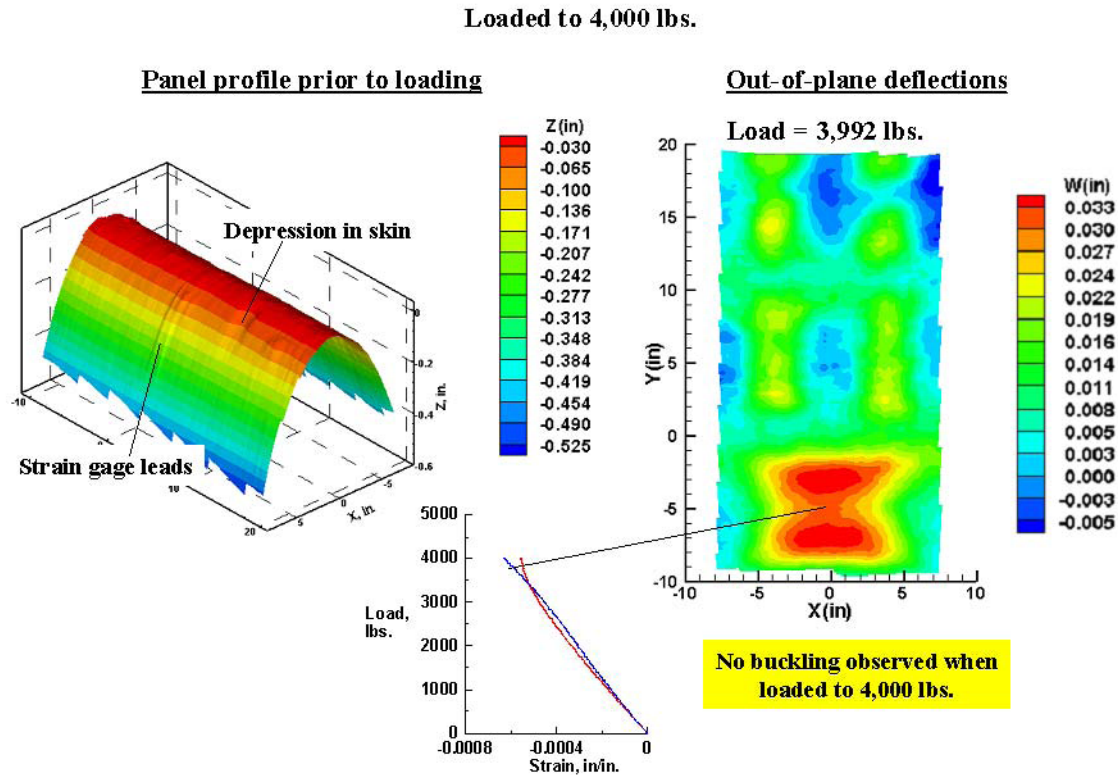


Figure 17. - First test on *Panel C-2*

Panel C-2 was reloaded to 4,500 lbs. The dashed lines shown on Figure 18 indicate the locations of the frames and stringers. The first buckle appeared at 4,150 lbs in the R/H bay as shown on the L/H side of Figure 18. The back-to-back strain gages 1 and 19 located at the upper R/H bay (just below

the buckle) also indicated a strain reversal at the buckling load. The skin in the lower bay bulges as in the first loading to 4,000 lbs. The panel was unloaded and removed from the test machine for impacting, prior to testing to failure.

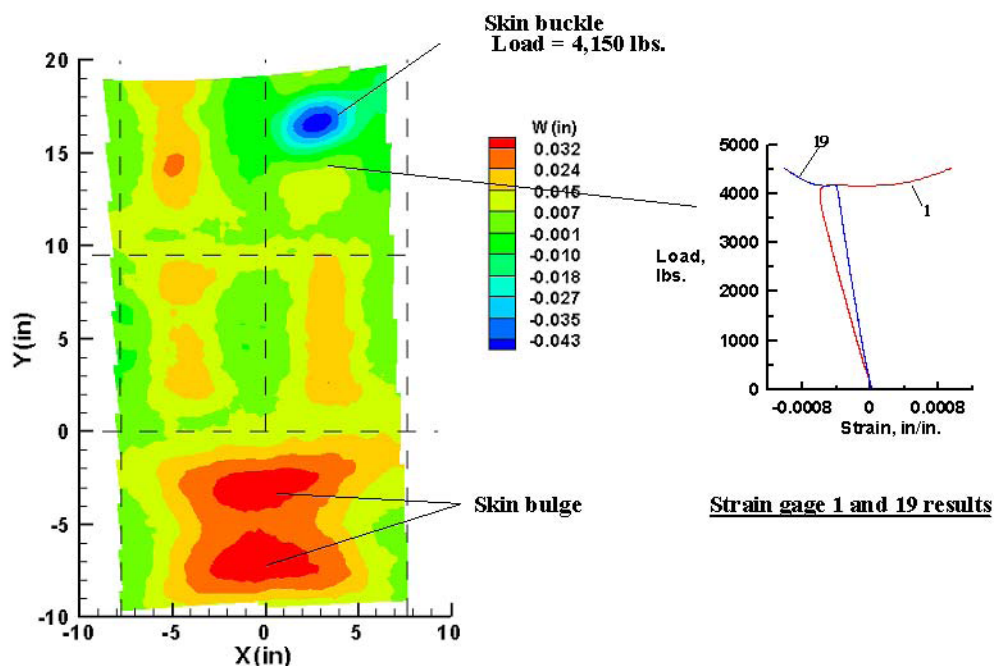
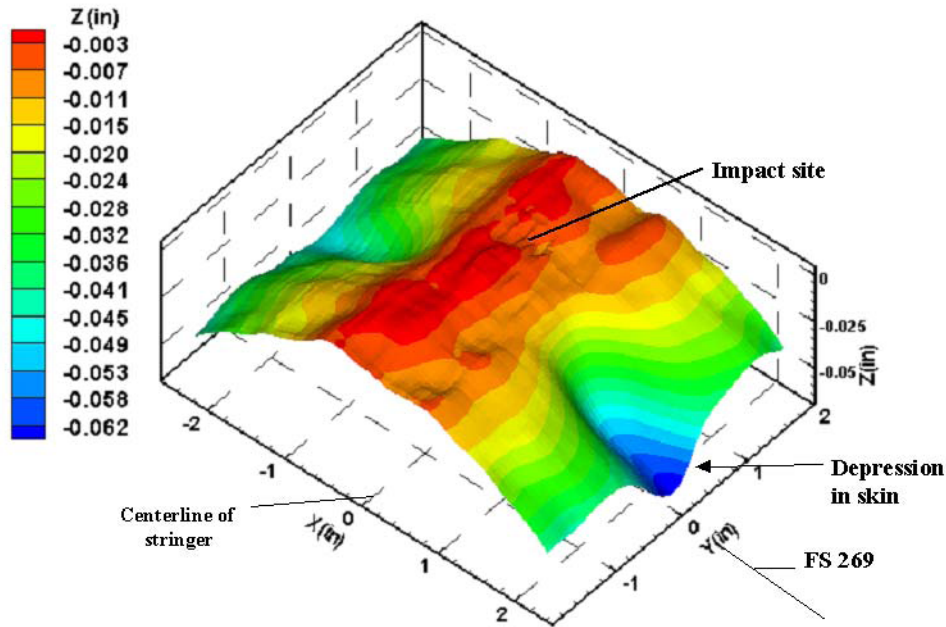


Figure 18. - Loading of *Panel C-2* to $N_y = 4,500$ lbs

Figure 19 shows the local VIC-3D system image of the area surrounding the impact site. The panel was impacted with 20 ft-lbs. of energy on the centerline of the panel, between the stringer termination and the frame flange at FS 269. There was no visible damage. The panel was impacted again at the same location with an energy level of 25 ft-lbs. The visible damage was slight compared to the damage of *Panel C-1*. A plot of the contact force versus time for the 25 ft-lb impact event is shown in Figure 20. The first peak of the contact force as a function of time curve occurred at 1,150 lbs. and then dropped to 750 lbs, recovered and reached a peak of 1,244 lbs. This behavior indicates the first contact force drop may be due to initiation of delamination. There was no perceptible stiffness loss as evidenced by the second peak.

The image shown Figure 19 was taken after the panel was reinstalled in the test machine. The image does not indicate any indentation from the two impacts as indicated in a previous figure for *Panel C-1*. It appears that there could be some surface fibers broken from the impacts. The skin depressions which were shown earlier in a profile of the complete panel are shown in more detail. The depressions are over the FS 269 frame and are approximately 0.020 in. below the surrounding surface.



17

Figure 19. - Local area view after impact.

After impact, *Panel C-2* was loaded in compression to failure. A perspective of the out-of-plane deformations at a load of $N_y = 7,242$ lbs. is shown in the top center of Figure 21. The sequence of events leading to the maximum load is as follows. The first buckle (blue area) developed in the upper R/H bay (see top L/H picture in the figure) at $N_y = 4,150$ lbs as noted earlier. A second buckle developed in the L/H side middle bay (see top R/H picture in the figure) near $N_y = 4,578$ lbs. Next the lower bay which had been bulging changed into an elliptical shaped area that is deflecting in the negative direction and a crescent shaped area deflecting in the positive direction (see lower L/H view in Figure 21) at $N_y = 4,765$ lbs. It would be difficult to call these two half-waves in the usual definition. The middle R/H bay continued to bulge out as the load increased. The upper L/H quadrant also bulged out as load increased until approximately $N_y = 6,000$ lbs. when it snapped into two half-waves. The deflections continued to increase as the load increased until the maximum load resulting in the deformed shape as shown in the top center of Figure 21.

Since the u , v , and w displacements are determined over the viewed area by the VIC 3-D system, it is possible to compute the strain components over the entire viewed surface. The longitudinal strain (ϵ_{yy}) for a load of $N_y = 7,242$ lbs is shown in the center of Figure 22. The snap through buckling that was shown in the previous figure in the three areas (upper R/H, middle L/H, and lower bay) is verified by the strain reversals for the same areas shown on this figure. The strains in the upper L/H bay start to diverge at approximately 3,000 lbs. as shown with very little change in the near side gage (22) as the load increases to $N_y = 6,000$ lbs. The jagged appearance of the curve for the far side gage (4) could

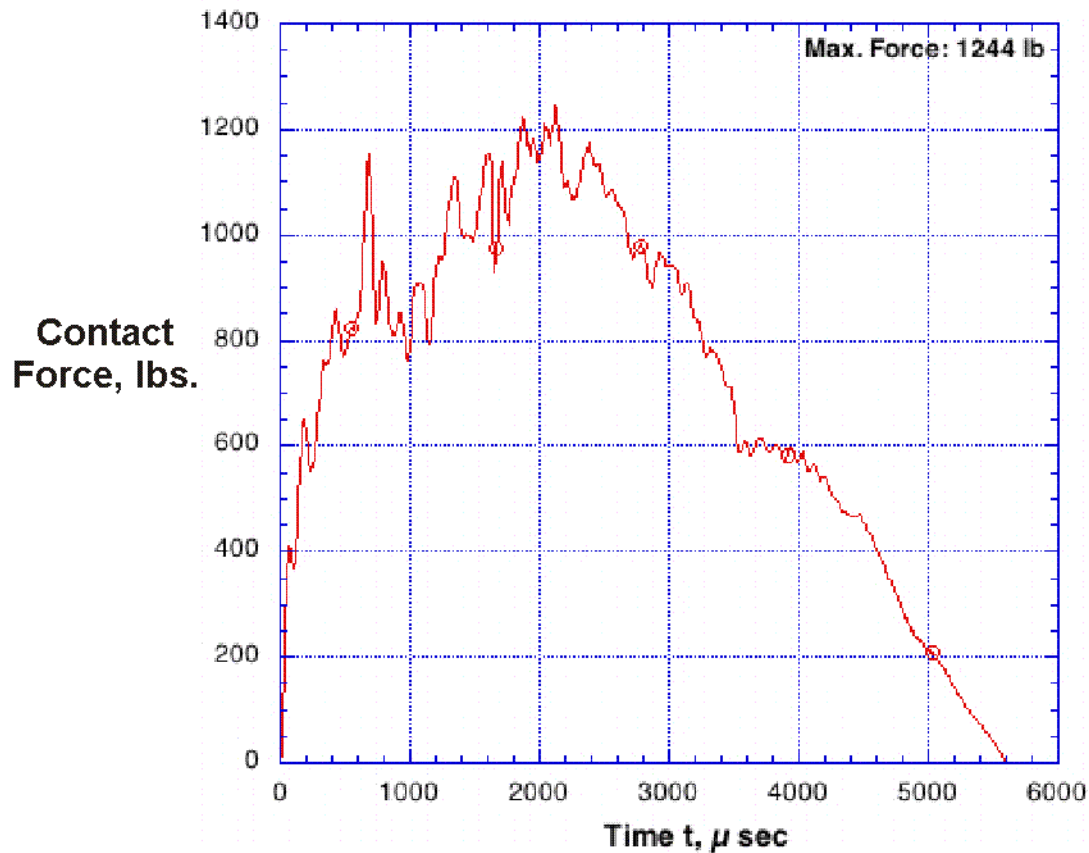


Figure 20. Contact force as a function of time for the 25 ft-lb impact.

indicate some failure is occurring on the far side surface as load increases from 4,000 to 5,000 lbs. After approximately 5,000 lbs. the compressive strain increases until both gages diverge farther at 6,000 lbs. The strain reversal in the upper L/H bay at approximately 6,000 lbs. is a snap through buckling as indicated previously. The irregular strain in the R/H middle bay as the load increases could be an indication of a failure initiation and is on the same side and between the frames that finally fail at the attaching point to the load reacting frame.

Comparison of the strain gage values from the high gage number in each pair of gages with the contours on the center figure indicates very good correlation between the computed strain from the displacement data and the strain gages.

A summary of some displacement results for *Panel C-2* are shown in Figure 23. The out-of-plane displacements shown on the L/H side of the figure are from a image taken near the failure load. The out-of-plane displacement pattern shown has the same features as the displacement shown previously at a load of 6,200 lbs. only with increased displacement values. The displacement result of a LVDT located in the middle of the lower bay is shown in the upper R/H side of the figure. The displacement reversal at 4,700 to 4,800 lbs. compares well with the VIC-3D system results. The LVDT is located on the panel centerline and near the end of the dark blue area shown in the image and there is good comparison between the results.

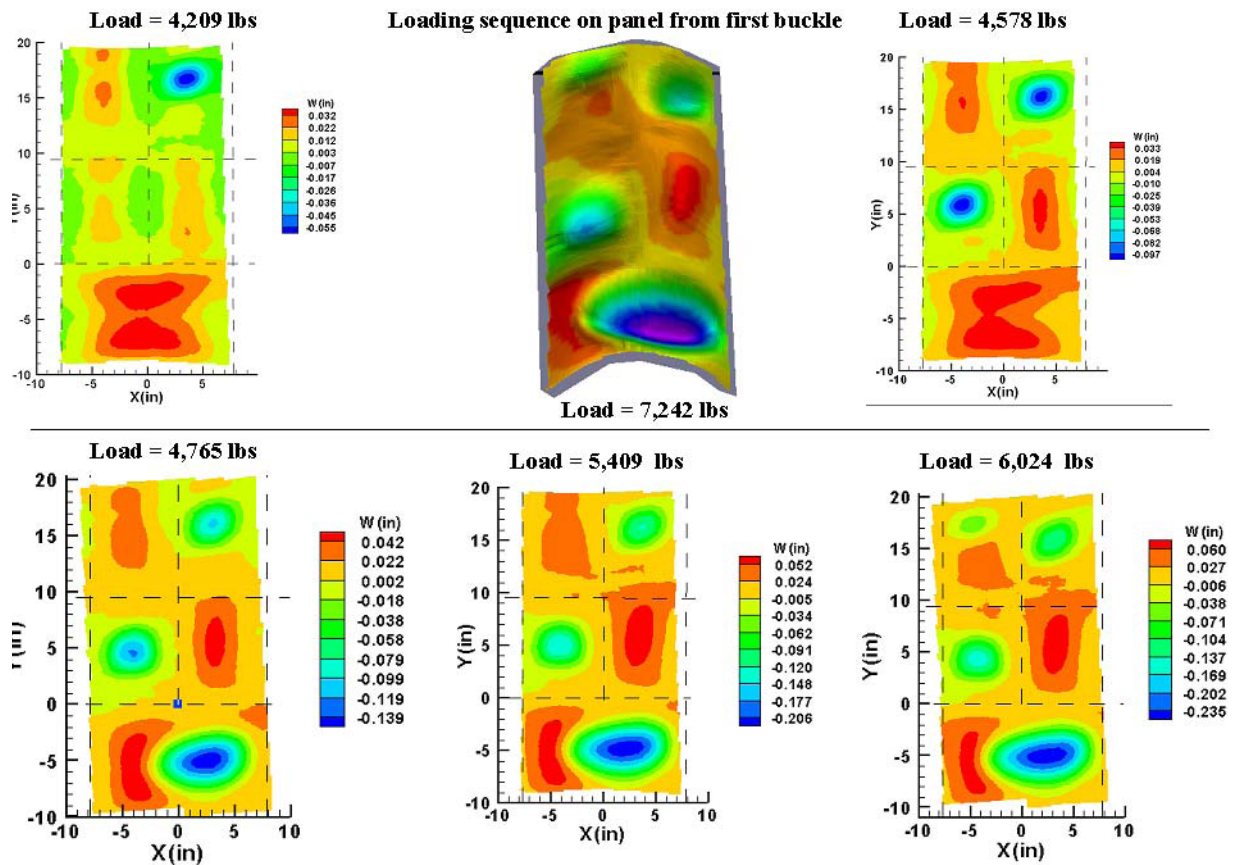


Figure 21. - Changes in the out-of-displacement as load increases on *Panel C-2*.

The load end shortening curve indicates a linear response until the initial buckle at approximately 4,100 lbs. then a constantly reducing slope (decreasing post-buckled stiffness) until failure. Panel stiffness loss from the impact was less than one percent. Post buckling stiffness of the panel was approximately 52 percent of the prebuckled stiffness.

Failure occurred at 7,266 lbs.

A recent version of VIC-3D software extracts more data from the images. Options exist that allow extraction of displacement and/or strain results at a point in the image or along a line on the image. The origin of the coordinate system for *Panel C-2* has been selected as the intersection of the center stiffener and the FS 269 as shown in Figure 24 on the out-of-plane displacement contour plot of for a load of $N_y = 7,242$ lbs. The points to determine the coordinate system are imbedded in the spackle pattern and require screen selection to determine the coordinate system. Selecting Line A through the impact site as shown in the Figure 24 will give the profile of the panel cross-section and the out-of-plane, w , displacements at 100 points (number of points selected by user) across the panel for a selected image/load. The location of this line is approximated by selecting two points on the screen. The profile across the panel at Line A after impact damage is shown in Figure 25 and indicates a surface irregularity near the center of the panel. The distances shown in the figure are the distance from a theoretical flat plane to the surface of the specimen. A review of a similar curve from the panel prior to impact testing indicates that surface irregularity was present prior to impact testing. This irregularity was also present in the VIC-3D

**Comparison of strain gages and strain computed
from data obtained from the VIC 3-D system**

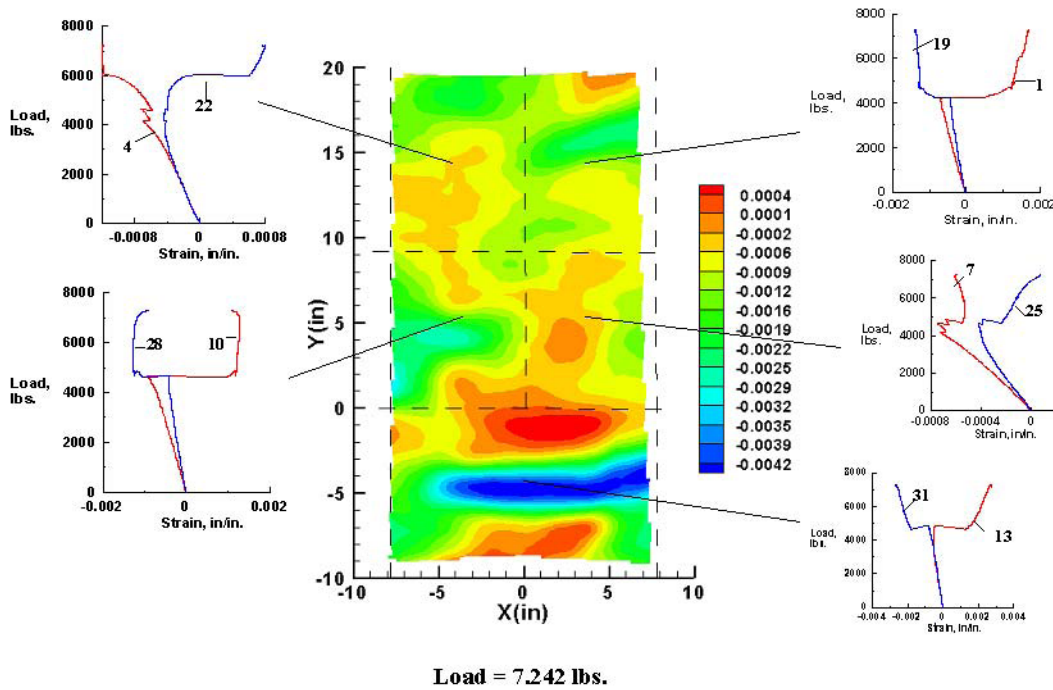


Figure 22. - Strains results at $N_y = 7,242$ lbs. on *Panel C-2*.

local profile view of the panel prior to testing. The out-of-plane displacement results at the location of Line A shown in Figure 24 are shown in Figure 26 for selected loads that vary from $N_y = 3,547$ lbs. to $N_y = 7,242$ lbs, which is the last image taken before failure. The green line with the triangle symbol ($N_y = 7,242$ lbs.) is the displacement from the last frame before maximum load. The line with the blue diamond symbol is at a load of $N_y = 7,136$ lbs. and is an image after maximum load. The curves shown in Figure 26 indicate the out-of-plane displacements vary across the panels which can only be seen with the full field capability of VIC-3D. Displacement transducers would only record a single point. The out-of-plane displacements indicate the panel appears to rotate about the edge at $x = 8.0$ inches until a load of approximately 5,000 lbs. The red curve with no symbols ($N_y = 5,409$ lbs) indicates the panel side at $x = 8.0$ -inches displaced approximately 0.03 inches from the previous curve ($N_y = 4,759$ lbs.) while the side at $x = -8.0$ -inches displaced approximately 0.007 inches. From this load until failure the panel again rotated about the side $x = 8.0$ as shown in Figure 26. Suspected failures at the frame attach points could be contributing to this panel rotation.

In addition the analysis software for VIC-3D allows the selection of a point on the image surface and determine the load-displacement history of the point. The load-displacement history for Point B (Figure 24) at the impact site on *Panel C-2* is shown in Figure 27 for loading to $N_y = 4,500$ lbs and loading to failure. This point is at or very near the impact site since it's location is determined by selecting a point on the screen. The deflection of the point prior to impacting when the panel was loaded to 4,500 lbs. is shown as the red line on Figure 27. Also shown is the load-displacement history of DCDT 16

Loading to failure

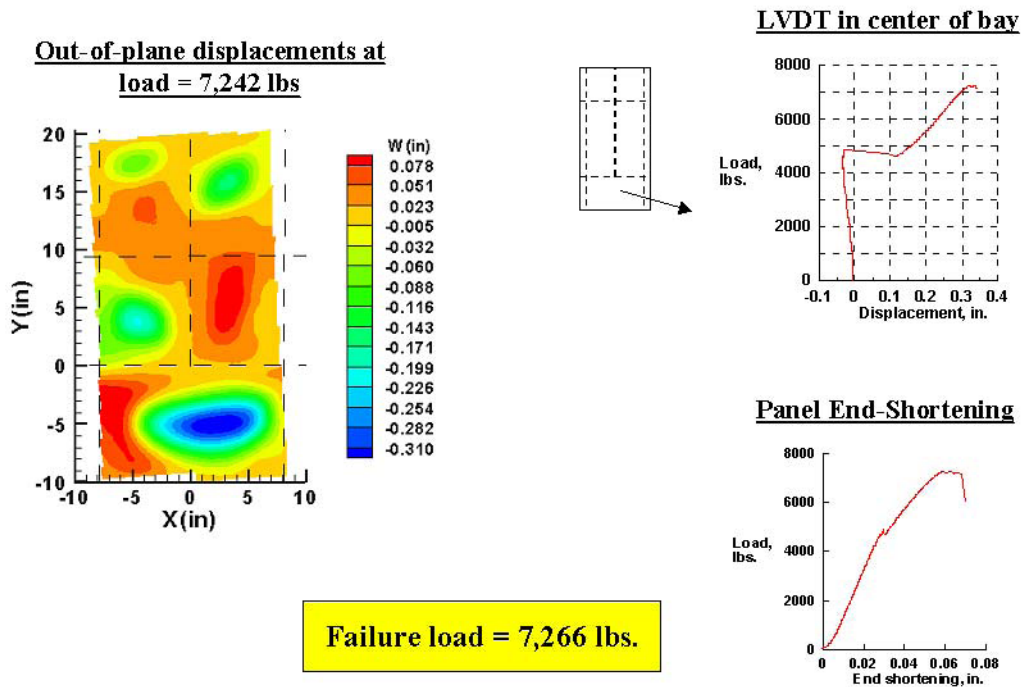


Figure 23. - *Panel C-2* out-of-plane displacement and end shortening.

which is located on the frame flange adjacent to the impact site. The three curves have the same trend, with the as expected lower displacement on a the frame flange which is a stiffer part of the structure. The curves indicate that the impact event has a slight effect on the panel surface deflection by reducing the stiffness.

The VIC-3D software also has the capability of extracting the strain at selected locations on the image. For *Panel C-2* the location selected to determine the strain is Line C as shown in Figure 24. Line C extends across the panel and intersects the strain gage rosette in the center of the bay with the results shown in Figure 28 for various load levels. The experimental results of the axial strain gage are shown for three load levels as symbols for the load levels enclosed by a circle. The gap in each group of symbols is the result of area of the image being removed for the rosette strain gage. The correlation between the strain gage and the VIC-3D curves is reasonable. It appears there is a small rotation in the coordination system since the strain gage results should be near the center of the gap. The strain gage is on the surface which has a high gradient which with a small difference in location can contribute to a large variation in the comparison of the results.

The failed *Panel C-2* is shown Figure 29. Close up views of the failure sites are shown and indicate the failure occurred around the attach points where the load reacting frame attached to the panel. The failures noted in the frame attach points are on the R/H side as shown in the image views on previous

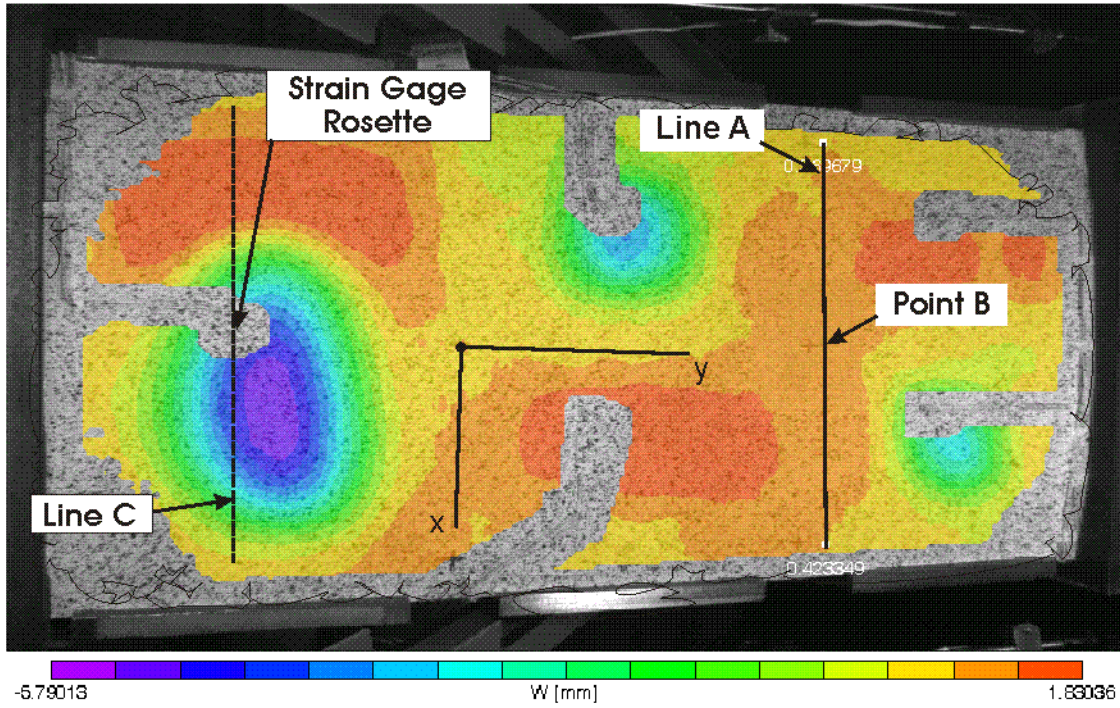


Figure 24. - Out-of-plane contour plot and location of selected strain and displacement results for *Panel C-2*.

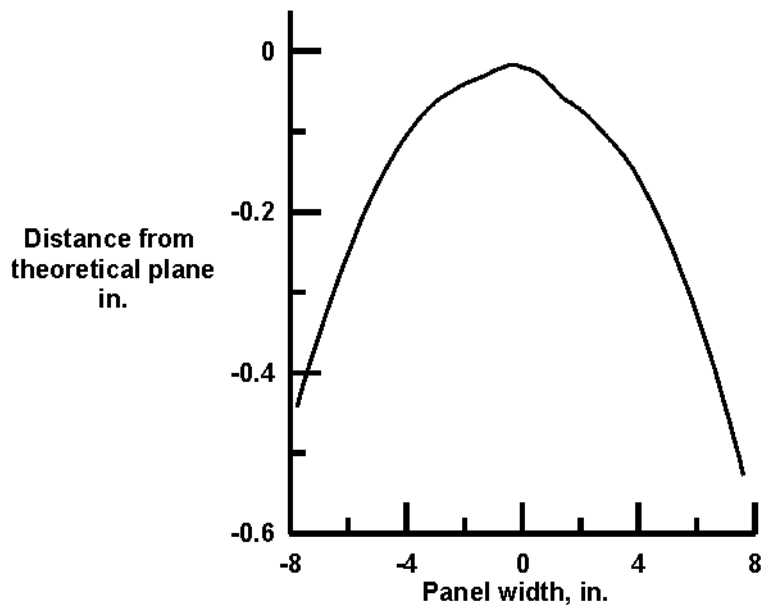


Figure 25. - Profile of *Panel C-2* across the panel at Line A.

figures. Figure 22 with strain results indicated unusual strain response in the R/H middle bay which could be the results of the frame starting to fail at approximately 4,100 lbs.

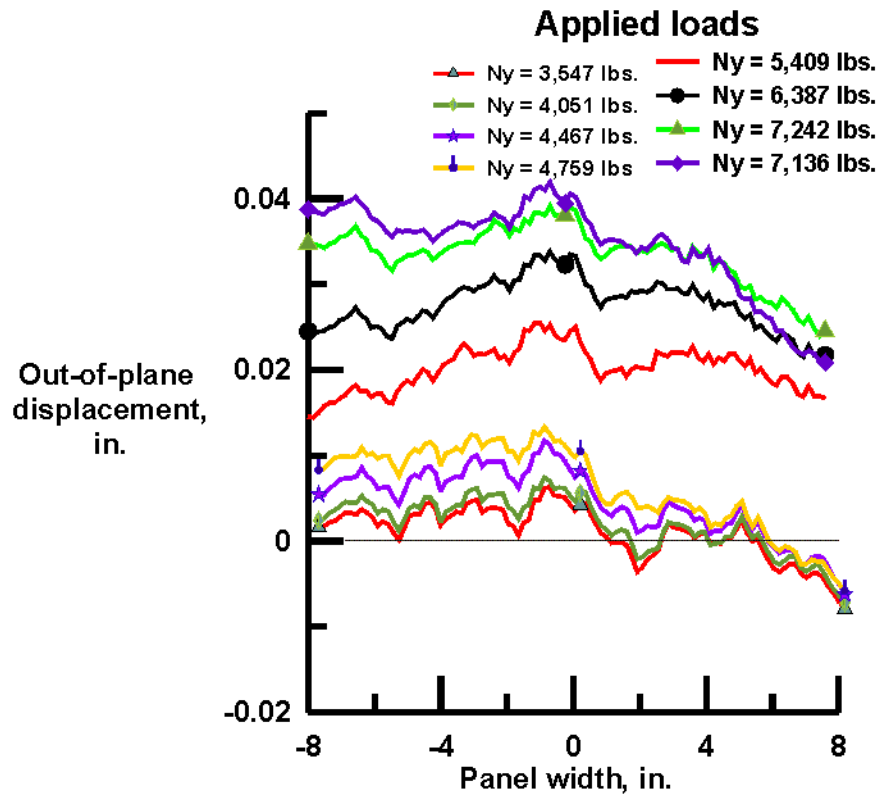


Figure 26. - History of out-of-displacement as a function of applied load.

It is impossible to determine if the failure of the frame attach points caused failure or if the bottom bay lost its load carrying ability from buckling allowing the panel to collapse.

Concluding Remarks

Two stitched VARTM multi-frame multi-stringer panels have been tested in uni-axial compression. The panels contained two frames and three stringers that divided the panels into 5 or 6 bays. The panel with 5 bays had the center stringer omitted between the frame and the end of the panel. The panels were 15.5-inches wide and 28.4-inches or 32.1-inches long. The stringers extended between the frames but did not go through the frames. The frame ends were supported to restrict the out-of-plane displacement only.

Panel response was recorded with strain gages and displacement transducers for determining the out-of-plane displacements. In addition a full-field-displacement measurement technique that uses a camera-based stereo-vision system was used to determine the displacements (u, v, w) in the skin. From these displacements the strains can be calculated.

The panels were loaded in increments to a predetermined load to determine the initial buckling, second bay buckling, etc. After reaching the desired load the panels were removed from the test machine and impacted on the centerline between the stringer termination and frame flange. Impact energy was 20 ft-lbs or 25 ft-lbs. With a 20 ft-lb impact one panel (5 bays) had no visible impact damage and the other panel (6 bays) had a 0.008-inch to 0.010-inch deep impact. The panel with five bays was impacted at 25 ft-lbs of energy and still did not sustain any visible damage. Panels were then returned to

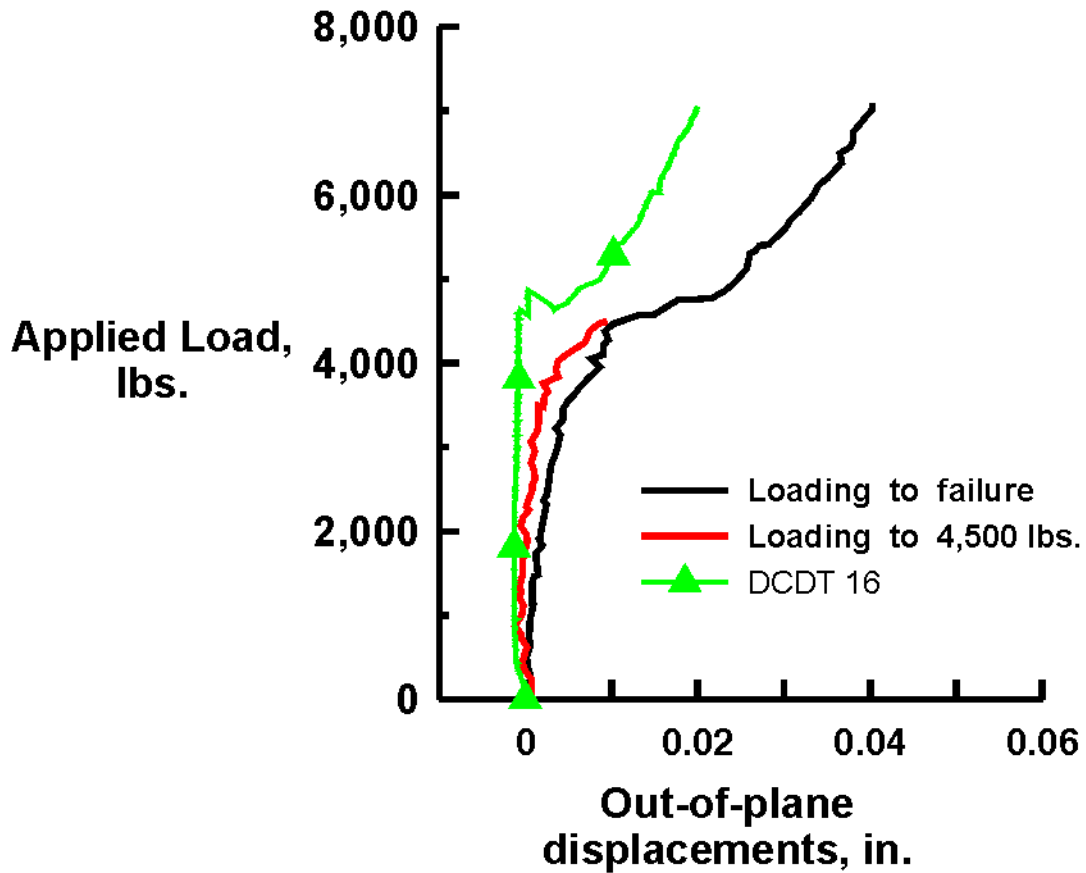


Figure 27. - Out-of-plane displacement at or near the impact point.

the test machine for loading to failure. Impact damage on the panel with 6 bays reduced the axial stiffness by 4 percent and the post buckled stiffness was 70 percent of the prebuckled stiffness. The panel with 6 bays failed by a frame rotating and the skin bending for the panel appear to be “folding” across the width of the panel. This “fold” in the panel intersected the impact site. Impact damage on the panel with 5 bays reduced the axial stiffness by less than one percent and the post buckled stiffness was 52 percent of the prebuckled stiffness. The panel with 5 bays failed in the panel frame where the frame attached to the frame for resisting translation. This panel also folded across the single bay.

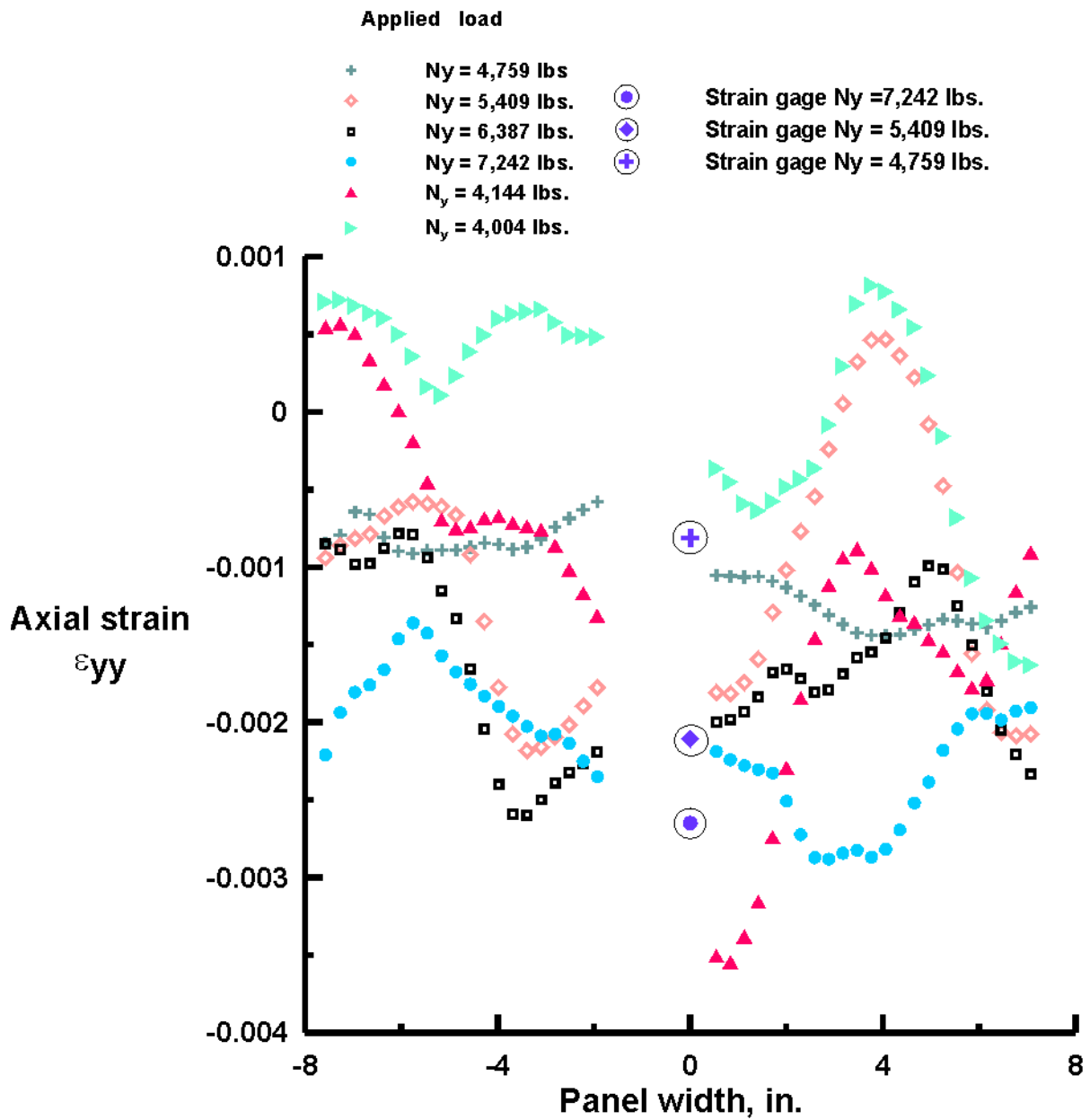


Figure 28. - History of strain distribution across bottom of *Panel C-2*.

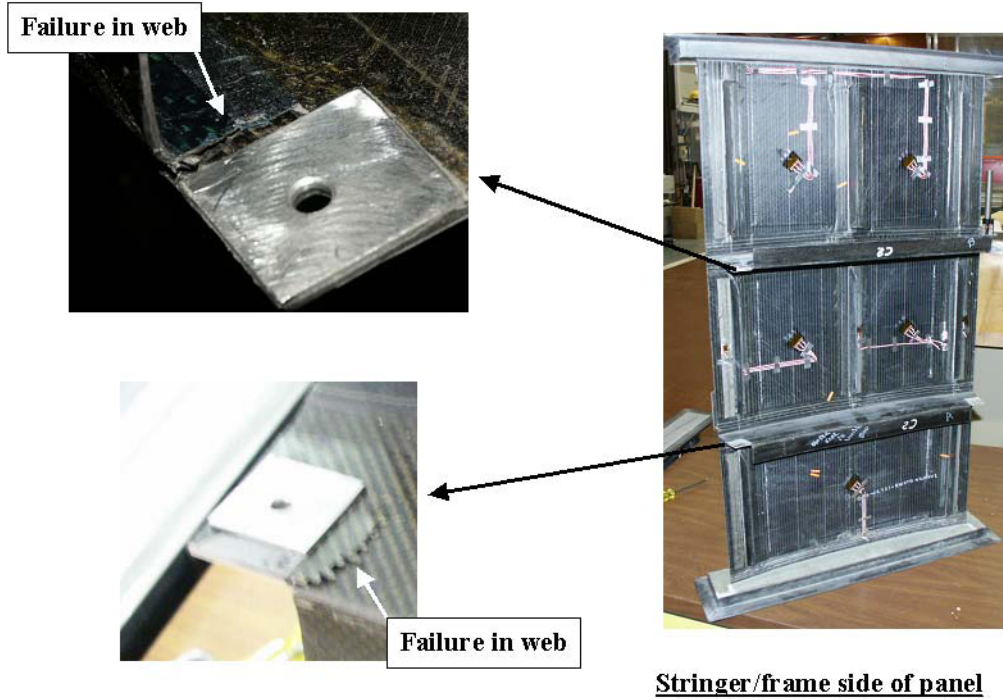


Figure 29 - Failed *Panel C-2*.

References

1. Helm, J.D., McNeil, S.R., Sutton, M.A., "Improved Three-Dimensional Image Correlation For Surface Displacement Measurement," *Optical Engineering*, Vol. 35, No 7, July 1996, pp1911-1920.
2. Li, J and Baker, Donald J., "Test and Analysis of a Composite Multi-bay Fuselage Panel Uni-axial Compression," *Proceedings of the 45th AIAA/ASME/AHS/ASC Structures, Structural Dynamics and Materials Conference, AIAA -2004-2056*, Palm Springs, CA, April 19-24, 2004.

REPORT DOCUMENTATION PAGE				Form Approved OMB No. 0704-0188	
<p>The public reporting burden for this collection of information is estimated to average 1 hour per response, including the time for reviewing instructions, searching existing data sources, gathering and maintaining the data needed, and completing and reviewing the collection of information. Send comments regarding this burden estimate or any other aspect of this collection of information, including suggestions for reducing this burden, to Department of Defense, Washington Headquarters Services, Directorate for Information Operations and Reports (0704-0188), 1215 Jefferson Davis Highway, Suite 1204, Arlington, VA 22202-4302. Respondents should be aware that notwithstanding any other provision of law, no person shall be subject to any penalty for failing to comply with a collection of information if it does not display a currently valid OMB control number.</p> <p>PLEASE DO NOT RETURN YOUR FORM TO THE ABOVE ADDRESS.</p>					
1. REPORT DATE (DD-MM-YYYY)		2. REPORT TYPE		3. DATES COVERED (From - To)	
01-09-2004		Technical Memorandum			
4. TITLE AND SUBTITLE Experimental Results From Stitched Composite Multi-Bay Fuselage Panels Tested Under Uni-Axial Compression				5a. CONTRACT NUMBER	
				5b. GRANT NUMBER	
				5c. PROGRAM ELEMENT NUMBER	
6. AUTHOR(S) Baker, Donald J.				5d. PROJECT NUMBER	
				5e. TASK NUMBER	
				5f. WORK UNIT NUMBER 23-719-55-TA	
7. PERFORMING ORGANIZATION NAME(S) AND ADDRESS(ES) NASA Langley Research Center Hampton, VA 23681-2199			8. PERFORMING ORGANIZATION REPORT NUMBER L-19031		
9. SPONSORING/MONITORING AGENCY NAME(S) AND ADDRESS(ES) National Aeronautics and Space Administration Washington, DC 20546-0001 and U.S. Army Research Laboratory Adelphi, MD 20783 -1145			10. SPONSOR/MONITOR'S ACRONYM(S) NASA		
			11. SPONSOR/MONITOR'S REPORT NUMBER(S) NASA TM-2004-213262 ARL-TR-3233		
12. DISTRIBUTION/AVAILABILITY STATEMENT Unclassified - Unlimited Subject Category 39 Availability: NASA CASI (301) 621-0390 Distribution: Nonstandard					
13. SUPPLEMENTARY NOTES An electronic version can be found at http://techreports.larc.nasa.gov/ltrs/ or http://ntrs.nasa.gov					
14. ABSTRACT The experimental results from two stitched VARTM composite panels tested under uni-axial compression loading are presented. The curved panels are divided by frames and stringers into five or six bays with a column of three bays along the compressive loading direction. The frames are supported at the ends to resist out-of-plane translation. Back-to-back strain gages are used to record the strain and displacement transducers were used to record the out-of-plane displacements. In addition a full-field measurement technique that utilizes a camera-based-stereo-vision system was used to record displacements. The panels were loaded in increments to determine the first bay to buckle. Loading was discontinued at limit load and the panels were removed from the test machine for impact testing. After impacting at 20 ft-lbs to 25 ft-lbs of energy with a spherical indenter, the panels were loaded in compression until failure. Impact testing reduced the axial stiffness 4 percent and less than 1 percent. Postbuckled axial panel stiffness was 52 percent and 70 percent of the pre-buckled stiffness.					
15. SUBJECT TERMS Composite Materials; Structural Mechanics					
16. SECURITY CLASSIFICATION OF:			17. LIMITATION OF ABSTRACT	18. NUMBER OF PAGES	19a. NAME OF RESPONSIBLE PERSON
a. REPORT	b. ABSTRACT	c. THIS PAGE			STI Help Desk (email: help@sti.nasa.gov)
U	U	U	UU	32	19b. TELEPHONE NUMBER (Include area code) (301) 621-0390